Journal of Sol-Gel Science and Technology (2020) 95:321–331
https://doi.org/10.1007/s10971-020-05239-6

ORIGINAL PAPER: SOL–GEL AND HYBRID MATERIALS FOR CATALYTIC, PHOTOELECTROCHEMICAL AND SENSOR APPLICATIONS

Titania-heteropolyacid composites (TiO_2-HPA) as catalyst for the green oxidation of trimethylphenol to 2,3,5-trimethyl-*p*-benzoquinone

Magdalena Palacio[1] · Paula I. Villabrille[1,2] · Valeria Palermo[1] · Gustavo P. Romanelli[1,2]

Received: 26 August 2019 / Accepted: 29 January 2020 / Published online: 10 February 2020

Abstract

New catalysts containing phosphomolybdic acid (PMA) and vanadophosphomolybdic acid (VPMA) in a titania matrix were synthesized by the sol–gel process with different heteropolyacid loads (5%, 15%, and 30% (w/w): 5PMA-TiO_2, 15PMA-TiO_2, 30PMA-TiO_2, 5VPMA-TiO_2, 15VPMA-TiO_2, and 30VPMA-TiO_2). The techniques used to characterize the materials were XRD, DRS, SEM, FT-IR, ^{31}P MAS-NMR, potentiometric titration with *n*-butylamine, and N_2 physisorption at −196 °C. The materials were used as heterogeneous catalysts in the oxidation of 2,3,6-trimethylphenol (TMP) to 2,3,5-trimethyl-*p*-benzoquinone (TMBQ), a key intermediate in vitamin E synthesis. The catalysts allowed an ecofriendly TMBQ synthesis, using ethanol as solvent and aqueous hydrogen peroxide as a clean oxidizing agent, at room temperature. The conversion of TMP reached 90% and 99% for the samples with 15PMA-TiO_2 and 15VPMA-TiO_2, respectively, after 4 h. The amount of Mo and V in the reaction medium was determined by ICP-MS, which showed leaching of only 17–18% Mo, but 48% V. Reuse of the catalysts was performed. For 15PMA-TiO_2, the conversion was maintained in the second cycle. A homolytic mechanism was proposed for TMBQ synthesis, which involved the formation of a peroxometallic species through an HPA-Ti center.

Graphical Abstract

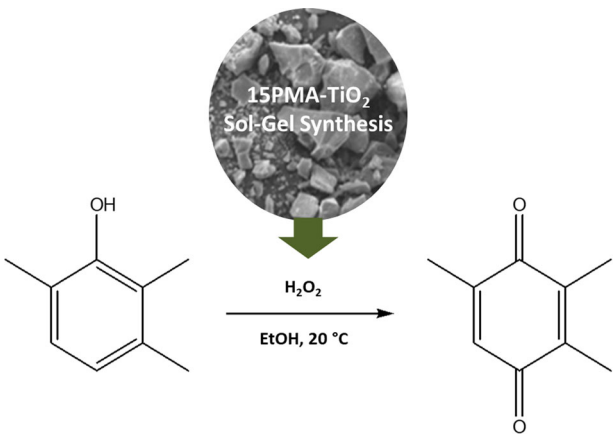

Keywords Titania-heteropolyacid composite · Sol–gel · Green oxidation · Hydrogen peroxide · Benzoquinone

✉ Valeria Palermo
vpalermo@quimica.unlp.edu.ar

[1] CINDECA (CONICET-CIC-UNLP), Dpto. Química, Facultad de Ciencias Exactas, Universidad Nacional de La Plata, Calle 47 No 257, B1900AJK La Plata, Argentina

[2] Dpto. Exactas, Facultad de Ciencias Agrarias y Forestales, Universidad Nacional de La Plata, Calles 60 y 119 s/n, B1904AAN La Plata, Argentina

Highlights

- Titania-heteropolyacid composites were obtained by the sol–gel method.
- The composites were tested as catalysts in the liquid phase oxidation of 2,3,6-trimethylphenol with aqueous hydrogen peroxide.
- For the catalyst with 15% phosphomolybdic acid, conversions of 90 and 85% were observed for the first and second cycles.
- The formation of a peroxometallic species through an HPA-Ti center was proposed as part of the homolytic mechanism.

1 Introduction

Heteropolyacids (HPAs) have been extensively studied as catalysts by many researchers. They have been used as acid and redox catalysts, especially for fine chemical synthesis, in academic research and industry [1], and to solve environmental issues such as toxic gas removal, wastewater treatment, corrosion, and radioactive waste processing [2]. In recent years, there has been a great deal of interest in the application of HPAs as homogeneous and heterogeneous catalysts, since they have several advantages such as inorganic nature, metal-oxide structure, and stability, which make them economically and environmentally attractive [3].

On the other hand, titania (TiO_2) has been one of the most widely studied supports for various catalytic reactions, mainly due to the high surface area, strong metal/support interaction, chemical stability, high conductivity, stability in acid-based media, and nontoxicity [4, 5]. Titania-supported HPA systems were used in dehydration reactions such as glycerol to acrolein [5] and methanol to dimethyl ether [6], synthesis of imidazoles [7], oxidation of phenols [8], in photocatalytic glucose oxidation [9], and degradation of dimethyl sulfide [10].

Different routes to prepare TiO_2-HPA composites have been investigated, for example HPAs were incorporated into TiO_2 colloids or TiO_2 suspensions, anchored to TiO_2 by chemical interactions or included during TiO_2 sol–gel synthesis [11]. Porous materials obtained by the sol–gel technique have optimal characteristics for fixing HPAs, providing surface properties to achieve suitable immobilization and catalytic ability. Each step in the sol–gel process can be controlled to obtain the best catalytic properties in the material [8].

A reaction of special interest is the oxidation of 2,3,6-trimethylphenol (TMP) for the production of 2,3,5-trimethyl-*p*-benzoquinone (TMBQ). This quinone has a key role in the synthesis of vitamin E (α-tocopherol) [12–14]. In addition, it is used as antioxidant in food, medicinal, and cosmetic treatments [14]. Vitamin E has proven to be the best biological fat-soluble antioxidant [15] and is particularly important to prevent the formation of hydroperoxide-derived polyunsaturated fatty acid [16].

There is a high global demand for vitamin E, and the cost to produce it on a large scale is huge, which has encouraged many researchers to develop a low-cost and fast procedure [17]. Many efforts have been reported to replace toxic and environmentally unfriendly inorganic oxidants, such as dichromate and permanganate [18], because most of them are stoichiometric reagents and generate huge amounts of waste. For this reason, environmentally benign oxidants such as molecular oxygen, hydrogen peroxide, and *t*-butyl hydroperoxide for the oxidation of TMP have been achieved using different catalysts. Kholdeeva and Zalomaeva [15] published a complete review with the main advances in this field. Among the catalysts reported to activate molecular oxygen, CuCl/LiCl (Mitsubishi G.C. process) [12], cobalt(II) complexes with salen, molecular copper(II) complexes, $Cu(OAc)_2$, complexes incorporated in molecular sieves [15], $Cu(NO_3)_2$ [19], and Keggin HPAs [20] stand out. Mitsubishi process required special corrosion-resistant apparatus for the large amounts of CuCl and produced chlorinated organic compounds as by-products [15]. Recently, HPAs supported on carbon nanotubes were also reported [21].

Organic catalytic oxidations with hydrogen peroxide (H_2O_2) are attractive because of its high content of active oxygen, low cost, and the fact that only water is obtained as by-product [22]. Although H_2O_2 is more expensive than molecular oxygen, the former has the advantage of easier activation that allows mild conditions and the use of simple and inexpensive technological equipment. Particularly, for the oxidation of TMP with H_2O_2 different catalysts were used: $FeCl_3$, $RuCl_3$, CH_3ReO_3, $Cu_2(OH)PO_4$, $CuCo_2O_4$ [15], titania-silica monoliths [23], silica-supported titania [24], titania-silica zeolite [13], TiO_2-SiO_2 xerogel [25], V_2O_5-TiO_2 mixed xerogels [8], divanadium- and dititanium-substituted γ-Keggin polyoxotungstates as tetra-*n*-butylammonium salt [26], and immobilized on nitrogen-doped carbon nanotubes [21] or supported on zeolites [17].

The general objective of this study is to explore new heterogeneous catalysts to carry out TMBQ synthesis. We propose the incorporation of Keggin HPAs during the sol–gel synthesis of TiO_2 to generate the active sites for the green oxidation reaction of TMP to TMBQ (Scheme 1).

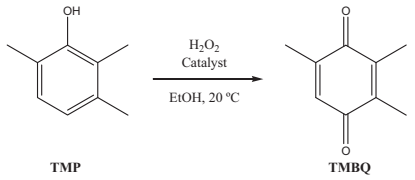

Scheme 1 Oxidation reaction of 2,3,6-trimethylphenol (TMP) to 2,3,5-trimethyl-*p*-benzoquinone (TMBQ)

2 Experimental

2.1 Catalyst synthesis

Phosphomolybdic acid (PMA, Fluka, 97%) or vanadophosphomolybdic acid (VPMA) prepared as previously reported [27] was immobilized in TiO_2 by the sol–gel technique using titanium(IV) isopropoxide (Aldrich, 97%) as precursor, and absolute ethanol (Aldrich, 99.8%) as solvent in a solvent/alkoxide molar ratio of 16, and was kept refluxing with continuous stirring. In addition, ethanolic HPA solutions were prepared according to the desired concentration of HPAs in TiO_2 (5%, 15%, or 30% (w/w)), and then added to the ethanol/alkoxide mixture. The pH was fixed to one with a 1 M nitric solution (HNO_3, Anedra). Finally, bidestilled water was added dropwise to achieve a water/alkoxide molar ratio of eight.

The reaction mixture was refluxed until the gel was formed. Then it was dried at 50 °C for 24 h to obtain the xerogel. Finally, it was calcined at 200 °C for 4 h.

The samples were labeled xPMA-TiO_2, with x as PMA% (w/w), and xVPMA-TiO_2 with x as VPMA% (w/w). In addition, a sample without HPAs (TiO_2) was prepared by a similar synthesis procedure for comparative purposes.

2.2 Catalyst characterization

2.2.1 Scanning electron microscopy with energy dispersive X-ray spectroscopy—SEM-EDAX

A Philips 505 scanning electron microscope was used with an accelerating voltage of 25 eV and a magnification of ×200. The samples had been previously metallized with gold. The chemical composition of the sample was analyzed by X-ray scattering.

2.2.2 Nuclear magnetic resonance spectroscopy—^{31}P MAS-NMR

Selected solid samples were analyzed by ^{31}P MAS-NMR in Bruker Avance II equipment. A proton decoupling continuous wave with a power equivalent to 31.25 kHz and a spin rate of 8 kHz were set. Phosphoric acid 85% was used as external reference.

2.2.3 Diffuse reflectance spectroscopy—DRS

The solid samples were analyzed in the range 200–800 nm, using a Perkin Elmer Lambda 35 UV–Vis double beam spectrophotometer with a scan rate of 240 nm/min and Spectralon as reference.

2.2.4 Fourier transform infrared spectroscopy—FT-IR

Thermo Bruker IFS 66 IR equipment was used to obtain the FT-IR spectra in transmission mode, in the range between 400 and 4000 cm^{-1}. The solid samples were dried, ground, and mixed with BrK to form a pellet (1% of sample).

2.2.5 X-ray diffraction—XRD

XRD patterns of solid samples were recorded by a Philips PW-1390 device with a built-in recorder, using Cu Kα radiation (λ = 1.5417 Å); Ni filter; 20 mA and 40 kV in the high voltage source; scanning angle (2θ) from 5° to 60°, scan rate of 2° (2θ)/min.

2.2.6 Textural properties

The nitrogen adsorption/desorption isotherms of the solids were determined by using Micromeritics ASAP 2020 equipment at −196 °C. Prior degasification was carried out for 700 min at 100 °C and below 30 mm Hg.

2.2.7 Acidity measurements

The total catalyst acidity was measured by potentiometric titration using 794 Basic Titrino device with a Solvotrode electrode. A solution of *n*-butylamine in acetonitrile (0.025 N) was used as the titrant at a flow rate of 0.025 cm^3/min. The sample (0.03 g) was suspended in 45 mL of acetonitrile and titrated under continuous stirring.

2.2.8 Catalytic oxidation reaction

Oxidation of TMP to TMBQ was performed in a glass reactor at room temperature (20 °C). The reaction mixture was composed of 2 mmol of TMP (Aldrich, 95%), 10 mL of ethanol (Soria, 96%), and 140 mg of catalyst. Then, 2 mL of aqueous hydrogen peroxide (Analquim, 73% (w/v), determined by iodometric titration) was added dropwise to the reaction mixture under vigorous stirring.

Samples of the reaction mixture (0.1 mL) were withdrawn at fixed intervals, and partitions with 0.5 mL of dichloromethane (ACS, 99.5%) and 0.5 mL bidistilled water were performed. The organic extract was dried on anhydrous sodium sulfate and analyzed by gas chromatography in a Shimadzu 2014 with a Supelco column (SPB-1,

30 m × 0.32 mm × 1 µm) and a flame ionization detector. TMP (Aldrich, 95%) and TMBQ (prepared and purified in our laboratory [8]) were used as standards.

After 4 h of reaction, the mixture was centrifuged, and the catalyst was separated, washed with ethanol and dried. Two catalysts (15PMA-TiO_2 and 15VPMA-TiO_2) were selected to test their reuse under the above reaction conditions.

To check the heterogeneous nature of the catalyst in the reaction medium, two tests were performed: (1) Test A: the catalyst was separated from the reaction solution after 30 min by centrifugation and subsequent filtration. Then, the reaction was continued without the catalyst, and the concentration of TMP was monitored. (2) Test B: the catalyst was kept in the reaction mixture (without TMP) for 4 h. Then, it was separated by centrifugation and subsequent filtration. Finally, TMP was added to the reaction mixture, and its concentration was determined during the next 4 h.

In order to study the catalyst/oxidant interaction, the assays were performed under the same previous conditions but without TMP. After 10 min the mixture was centrifuged and filtered to separate the catalyst. The obtained solids were dried, and their diffuse reflectance spectra were recorded.

On the other hand, in order to study whether the reaction mechanism could be homolytic or heterolytic, the oxidation of TMP to TMBQ was performed using a free-radical inhibitor (*t*-butanol).

2.2.9 Inductively coupled plasma mass spectrometry–ICP-MS

The presence of Mo and/or V in the reaction mixture was determined by ICP-MS. A NexION 300X ICP mass spectrometer instrument (Perkin Elmer) was used. Calibration curves were made from a standard solution certified by Perkin Elmer. The detection limit was of few parts per trillion for each metal.

3 Results and discussion

3.1 Catalyst characterization

EDAX revealed the presence of Ti, P, Mo, and V in all the samples. As an example, Fig. 1 compares the spectra of TiO_2, 15PMA-TiO_2, and 15VPMA-TiO_2. As shown in the SEM images of Fig. 1, the morphology and size of TiO_2 are irregular and do not significantly change after HPA incorporation.

The ^{31}P MAS-NMR spectra of PMA and VPMA (Fig. 2) show a chemical shift at −3.8 ppm and −4 ppm, respectively. This line can be assigned to the presence of P-OH group associated with the Keggin unit of phosphomolybdate [28]. In Fig. 2 it can be observed that the signals shift to downfield and show a line broadening with the increment of HPA content. This could be attributed to the interaction between titania and Keggin polyanion. The presence of a single peak that appears for HPA/TiO_2 materials indicates that the Keggin structure remains intact [11].

The DRS spectra of the prepared materials present the typical broad bands reported for TiO_2: 200–400 nm is associated with the charge transfer of tetrahedral titanium sites, and 260–330 nm corresponds to octahedral titanium [29]. This band is overlapped with the band assigned to $O^{2-} \rightarrow Mo^{6+}$. The extended band beyond 400 nm suggests the presence of the intact Keggin unit (Fig. 3) [30]; this red shift is most important for vanadium-containing materials, in concordance with previous results [27].

In the FT-IR spectra of solids with increasing content of PMA or VPMA (Fig. 4) a shoulder appears between 1100 and 950 cm^{-1}, which could be attributed to the bands corresponding to the stretching of P–O_a and Mo=O_t of the Keggin structure. This indicates that the Keggin structure of HPAs remains unchanged after incorporation in a titania matrix, in agreement with ^{31}P MAS-NMR and DRS results.

The presence of a signal at 1633 cm^{-1} is due to the OH groups [8]. Besides, two bands at 1525 and 1434 cm^{-1} are distinguished, which are only present in catalysts containing HPAs; these bands could probably originate from Ti-HPA interaction.

X-ray diffraction patterns of the samples are presented in Fig. 5. It can be seen that solids containing 5% (w/w) of HPAs have a degree of crystallinity similar to TiO_2, with characteristic anatase phase peaks [8]. The main 2θ peaks at 25.30°, 37.90°, 48.10°, and 54.20° are identified. The diffraction patterns of solids containing 15% and 30% (w/w) HPAs are typical of amorphous material.

The N_2 adsorption/desorption isotherms for the samples with different concentrations of PMA and VPMA can be classified as Type IV according to IUPAC, characteristic of a mesoporous solid (Fig. 6). The addition of different amounts of HPAs to titania influences pore characteristics. TiO_2 and 5PMA-TiO_2 present H2-type hysteresis loops, which is attributed to effects of pore connectivity resulting from the presence of pores with narrow openings. However, when the PMA amount is high (15PMA-TiO_2 and 30PMA-TiO_2) the hysteresis loop shape changes, as can be seen in Fig. 6a, with a tendency to H4-type hysteresis loops, with horizontal adsorption/desorption branches associated with narrow slit-shaped pores. Catalysts containing VPMA (Fig. 6b) exhibit isotherms with the same characteristics as the corresponding analogs containing PMA.

The specific surface area (S_{BET}) values determined from the isotherms are listed in Table 1. The HPA inclusion in the TiO_2 structure produces a strong increase in the S_{BET}

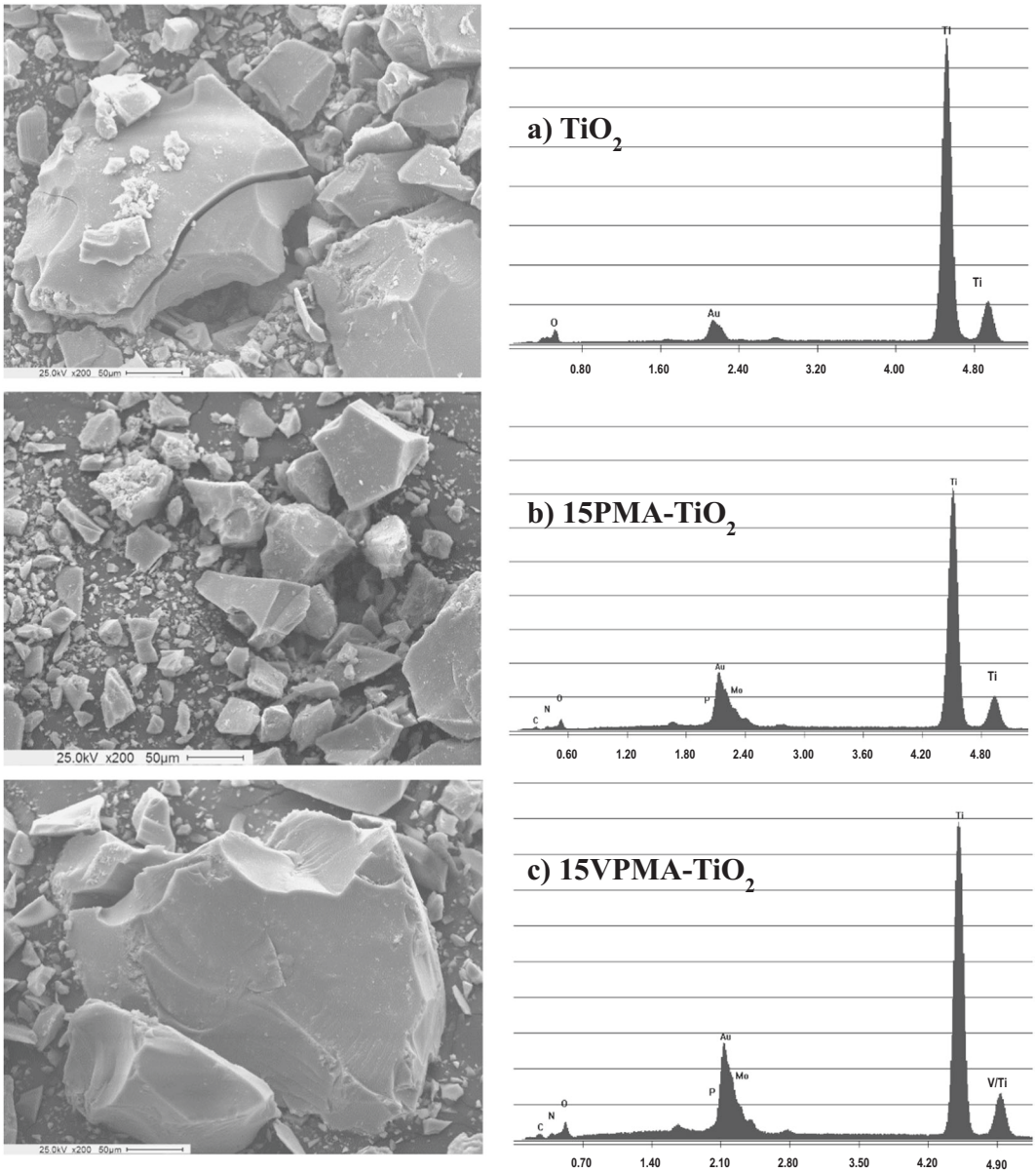

Fig. 1 SEM micrographs (×200) and EDAX spectra of (**a**) TiO_2, (**b**) 15PMA-TiO_2, and (**c**) 15VPMA-TiO_2

with the highest value obtained for 15% (w/w) HPAs, 383 m^2/g and 369 m^2/g for 15PMA-TiO_2 and 15VPMA-TiO_2, respectively. It can be seen that the surface area increases with the increment of HPAs until 15% (w/w), and then decreases. This can be attributed to pore formation after HPA additions in xerogel synthesis, since a small presence of HPAs prevents the compression of titania skeleton during the drying of the gel [31].

The total acidity of xHPA-TiO_2 was determined by potentiometric titration (Fig. 7). The incorporation of HPA, a very strong acid, into TiO_2 increased the acid strength. In comparison with bulk HPA, the catalysts presented a lower acid strength because the HPA protons were involved in the interaction with TiO_2. To interpret the potentiometric titration results, it is suggested that the initial electrode potential (E_0) indicates the maximum acid strength of the surface sites (Table 1). The acid strength of surface sites (E_0) has been classified as: very strong site $E_0 > 100$ mV; strong site $0 < E_0 < 100$ mV; weak site $-100 < E_0 < 0$ mV; very weak site $E_0 < -100$ mV [32]. According to the acid strength, TiO_2 and xHPA-TiO_2 materials have very strong sites.

3.2 Catalytic oxidation reaction

The catalytic activity of the prepared materials was determined for the oxidation reaction of TMP to TMBQ

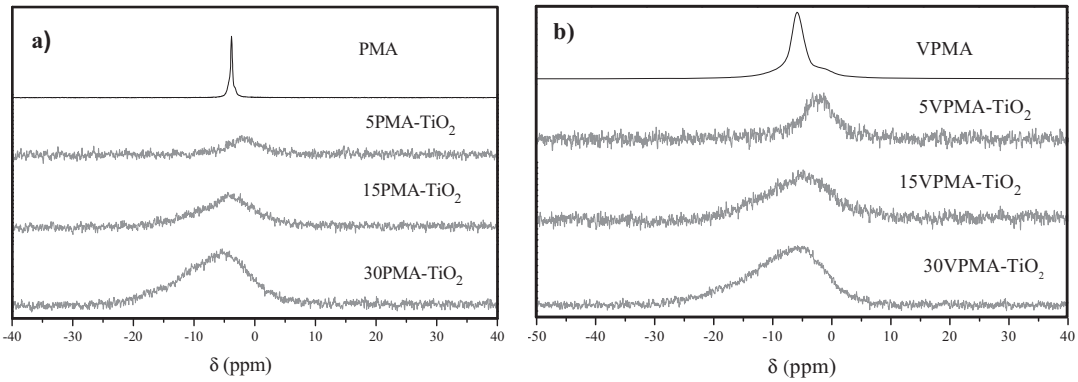

Fig. 2 ^{31}P MAS-NMR spectra of (**a**) xPMA-TiO_2 and (**b**) xVPMA-TiO_2

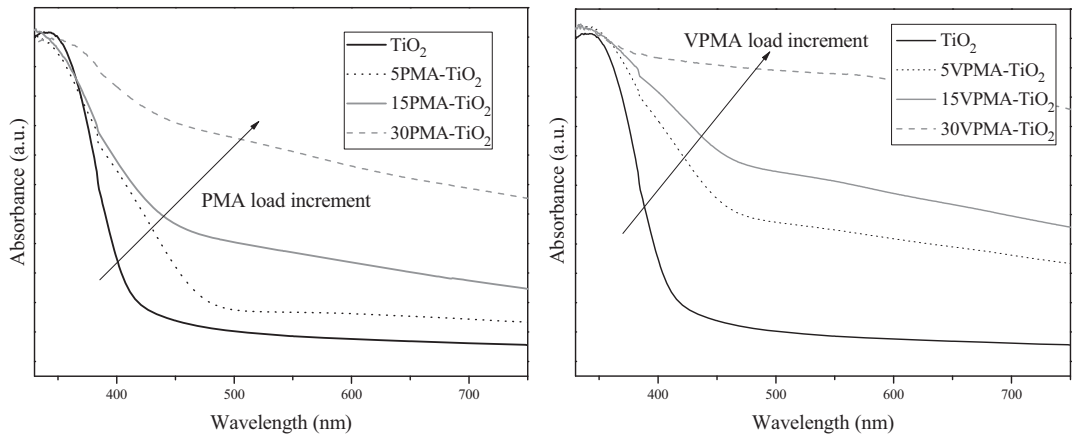

Fig. 3 DRS spectra of xPMA-TiO_2 and xVPMA-TiO_2

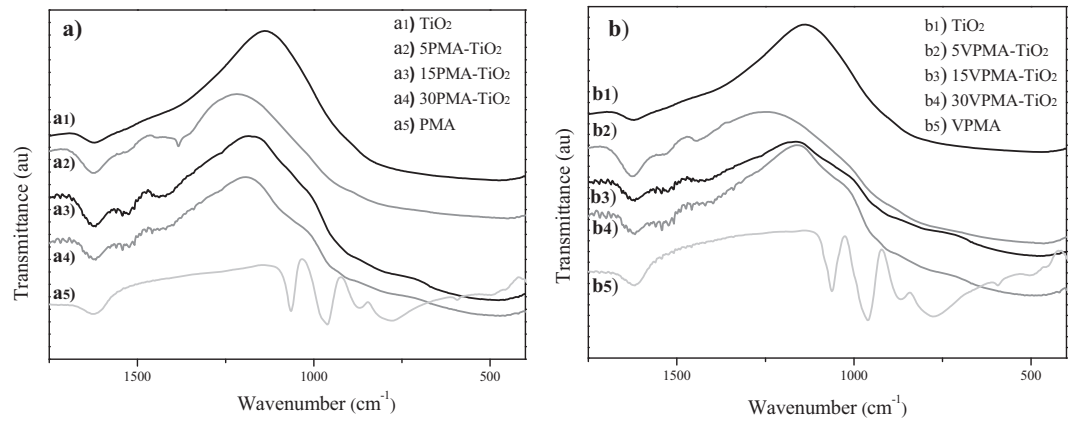

Fig. 4 FT-IR spectra of (**a**) xPMA-TiO_2 and (**b**) xVPMA-TiO_2

(Scheme 1). The effect of HPA nature (the presence of vanadium) and the amount of the active phase in the material on the catalytic activity in TMP oxidation was analyzed. The conversions achieved after 4 h of reaction with the different catalysts are listed in Table 1. The selectivity to TMBQ was 100% for all the catalysts.

A blank test was carried out without the catalyst; no TMP conversion was observed after 4 h of reaction. And using TiO_2 a conversion lower than 8% was obtained after 4 h of reaction (Table 1, Entry 1).

It can be observed that the addition of HPA to the material increases the conversion of TMP, reaching a

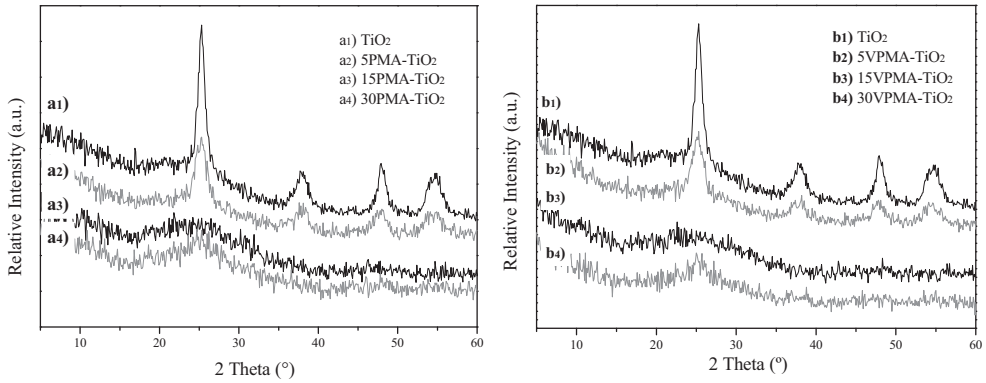

Fig. 5 XRD patterns of (**a**) x-PMA-TiO_2 and (**b**) x-VPMA-TiO_2

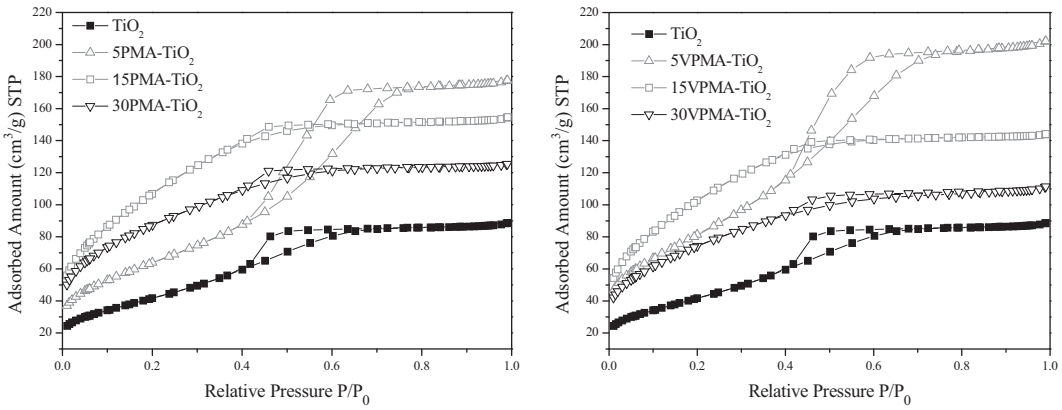

Fig. 6 Adsorption/desorption isotherms of N_2 on (**a**) xPMA-TiO_2 and (**b**) xVPMA-TiO_2

Table 1 Textural properties, acidity, and TMP conversion for the catalysts

Entry	Catalyst	S_{BET}[a] (m^2/g)	E_0[b] (mV)	Conv.[c] (%)
1	TiO_2	148	99	7.3
2	5PMA-TiO_2	227	183	34.8
3	15PMA-TiO_2	383	187	89.5 (84.6[d])
4	30PMA-TiO_2	312	205	66.7
5	5VPMA-TiO_2	289	112	48.8
6	15VPMA-TiO_2	369	264	98.5 (50.2[d])
7	30VPMA-TiO_2	265	221	87.4

[a]Specific superficial area obtained from nitrogen adsorption/desorption isotherms

[b]Maximum acid strength (initial electrode potential) determined by potentiometric titration

[c]Reaction conditions: TMP (2 mmol); catalyst (140 mg); ethanol (10 mL); H_2O_2 (73.5% (w/v), 2 mL); temperature, 20 °C; time, 4 h; stirring. The crude product was recrystallized. The selectivity to TMBQ was 100% for all the catalysts

[d]Second run

maximum value when the concentration is 15% (w/w). The lower activity of 30HPA-TiO_2 could be due to the fact that catalytic centers are not accessible to substrates (because of their lower surface area).

In this study, TMP conversion with xVPMA-TiO_2 as catalyst increased with respect to the use of xPMA-TiO_2 (Table 1), which is in agreement with several previous studies of oxidation reactions using bulk PMA and VPMA [33, 34]. This could be explained since the replacement of molybdenum by vanadium in the Keggin unit increased the potential reduction and the catalyst acidity [27, 35, 36].

The best performance was achieved with 15HPA-TiO_2, with a conversion close to 100%, so these catalysts were chosen to study their reuse. For these assays, the catalysts were isolated from the reaction medium, washed with ethanol, dried and used under the same reaction conditions. The conversion was maintained for 15PMA-TiO_2 after 4 h (Table 1, Entry 3) but decreased significantly for 15VPMA-TiO_2 (Table 1, Entry 6). This result could be attributed to a possible vanadium species leaching [21, 35].

The concentrations of Mo and V in the reaction mixture were tested by ICP-MS. The obtained values were 0.301 ppm Mo for 15PMA-TiO_2 and 0.303 ppm Mo and

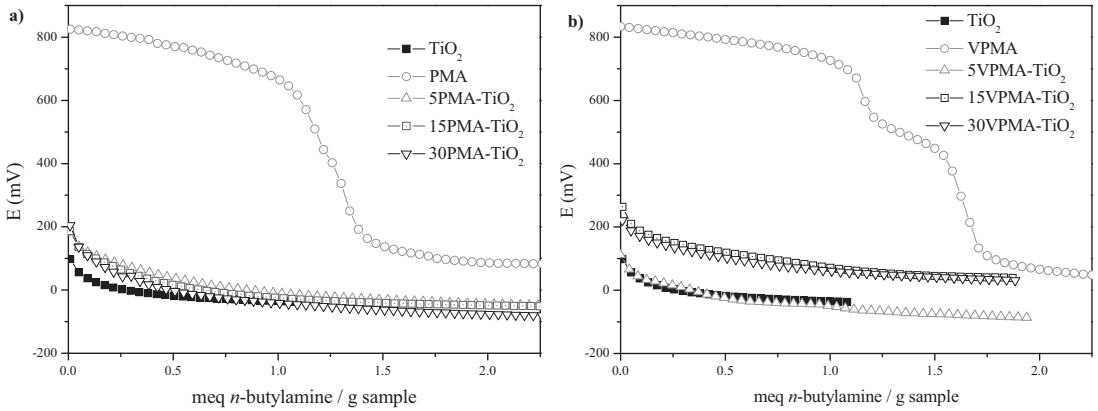

Fig. 7 Potentiometric titration with *n*-butylamine (**a**) xPMA-TiO_2 and (**b**) xVPMA-TiO_2

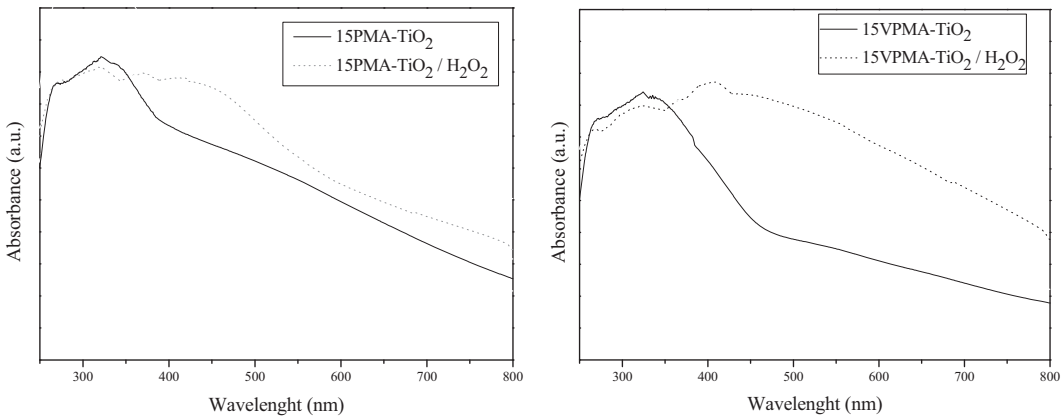

Fig. 8 DRS spectra of the 15HPA-TiO_2 catalysts before and after being in contact with H_2O_2

0.00382 ppm V for 15VPMA-TiO_2. These values represent a leaching of 48% of V and only 17% and 18% of Mo under the reaction conditions for 15PMA-TiO_2 and 15VPMA-TiO_2, respectively.

To study if the process is heterogeneous, some tests were performed. No TMP conversion was observed after 4 h of reaction with bulk PMA (22 mg). In addition, only 5% of TMP conversion was reached using bulk PMA (22 mg) and TiO_2 (122 mg) together in the reaction mixture, a similar value to that obtained with TiO_2 (Table 1, Entry 1). Then it could be assumed that the active site is formed during the catalyst synthesis.

In addition, two tests (A and B) were run using the catalyst with the best performance: 15PMA-TiO_2. The conversion of TMP was lower than 20% when the catalyst was removed after 30 min (Test A), and it was still lower when TMP was added after removing the catalyst (Test B). Then, we can assume the true heterogeneous nature of the 15PMA-TiO_2 catalyst, although a small percentage of Mo was leached under the reaction conditions (according to Mo ICP measurements).

3.3 Possible mechanism of the oxidation reaction

When the reaction was performed using a free-radical inhibitor, *t*-butanol as the reaction solvent, and 15PMA-TiO_2 as catalyst, TMP conversion was inhibited, reaching only 12% after 4 h. This result suggests that the mechanism could correspond to a homolytic oxidation [8].

An assay was done to study the oxidant/catalyst interaction. As shown in Fig. 8, the DRS spectra of the solids that were in contact with H_2O_2 showed a bathochromic shift of the absorption band. This shift could be caused by σ-σ * and π-σ * charge transfer metal-ligand transitions of the titanium peroxide complex [37]. The formation of a peroxometallic species usually involves d^0 transition metallic elements and hydrogen peroxide, as was reported previously [38].

A possible mechanism is proposed in Scheme 2. It involves TMP chemisorption on an HPA-Ti center [39], the hydroxylation and activation of H_2O_2 through the formation of a titanium hydroperoxo species, the subsequent homolytic cleavage, and the electrophilic oxygen atom transfer to

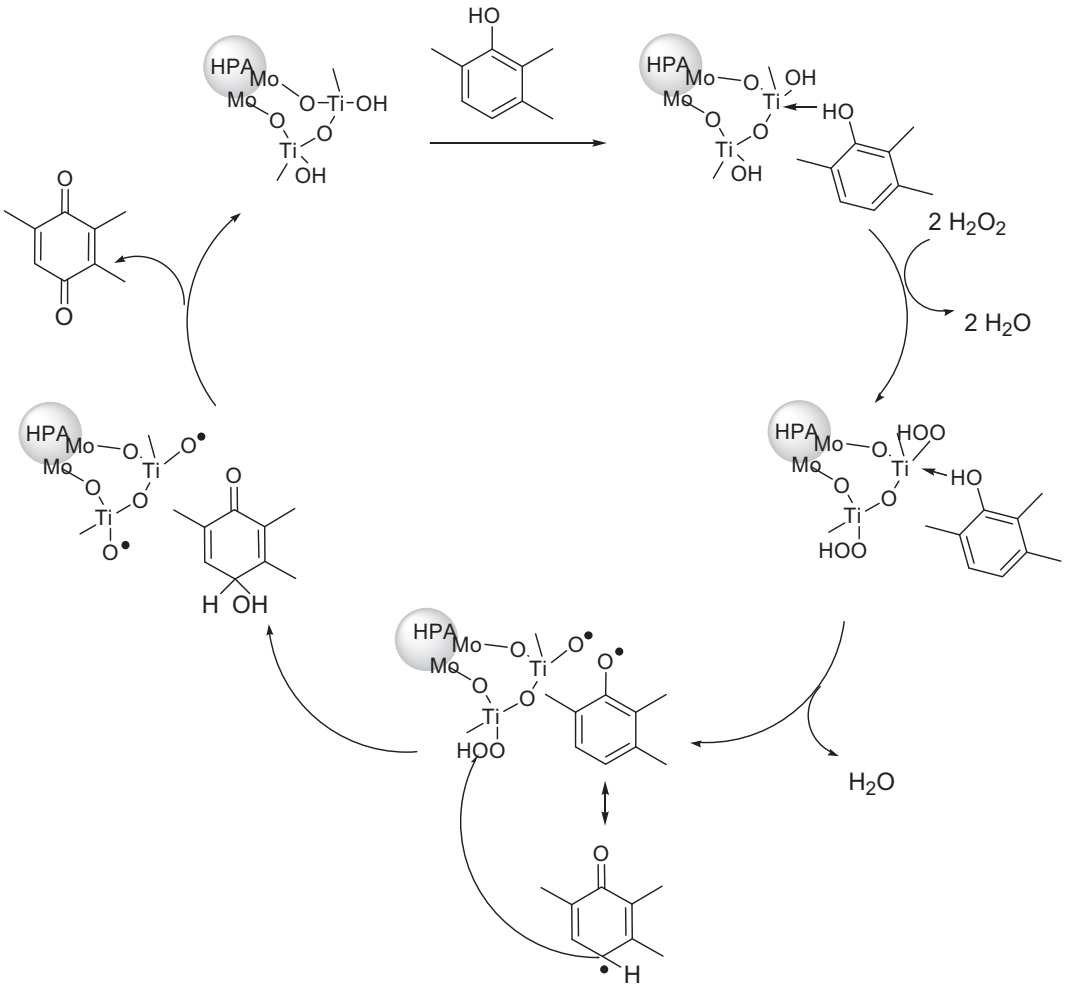

Scheme 2 Possible mechanism of the oxidation reaction

TMP at *para* position to achieve the TMBQ by an oxidative dehydrogenation [15].

4 Conclusions

New titania-Keggin heteropolyacid (PMA and VPMA) composites were synthesized by the sol–gel process. The presence of Keggin structure in the catalysts was corroborated by different techniques. The catalytic activity was tested for TMP oxidation to TMBQ at room temperature in ecofriendly media: aqueous H_2O_2 solution and ethanol.

A homolytic mechanism was proposed, which involved the formation of a peroxometallic species through an HPA-Ti center. The TMP oxidation with H_2O_2 over xHPA-TiO_2 reached 100% selectivity to TMBQ. The optimal TMP conversion was achieved with the catalysts containing 15% HPAs in a TiO_2 matrix. The catalysts can be easily isolated from the reaction media and reused in a new run, with good activity.

In conclusion, 15PMA-TiO_2 is a good catalyst to prepare TMBQ, an intermediate of vitamin E, using a simple and safe methodology.

Acknowledgements The authors thank CONICET and UNLP for their financial support; and Dr José J. Martínez Zambrano for his collaboration in the discussion of results.

Compliance with ethical standards

Conflict of interest The authors declare that they have no conflict of interest.

References

1. Heravi MM, Sadjadi S (2009) Recent developments in use of heteropolyacids, their salts and polyoxometalates in organic synthesis. J Iran Chem Soc 6:1–54

2. Omwoma S, Gore CT, Ji Y, Hu C, Song Y-F (2015) Environmentally benign polyoxometalate materials. Coord Chem Rev 286:17–29
3. Kholdeeva OA, Maksimchuk NV, Maksimov GM (2010) Polyoxometalate-based heterogeneous catalysts for liquid phase selective oxidations: comparison of different strategies. Catal Today 157:107–113
4. Bagheri S, Muhd Julkapli N, Bee Abd Hamid S (2014) Titanium dioxide as a catalyst support in heterogeneous catalysis. Sci World J 2014:1–21
5. Kang TH, Choi JH, Gim MY, Choi JS, Joe W, Song YK (2016) Dehydration of glycerin to acrolein over $H_3PW_{12}O_{40}$ catalyst supported on mesoporous titania. J Nanosci Nanotechnol 16:10829–10834
6. Ladera RM, Garcia Fierro JL, Ojeda M, Rojas S (2014) TiO_2-supported heteropoly acids for low-temperature synthesis of dimethyl ether from methanol. J Catal 312:195–203
7. Shamsi T, Amoozadeh A, Tabrizian E, Sajjadi SM (2017) A new zwitterionic nano-titania supported Keggin phosphotungstic heteropolyacid: an efficient and recyclable heterogeneous nanocatalyst for the synthesis of 2,4,5-triaryl substituted imidazoles. Reac Kinet Mech Cat 121:505–522
8. Palacio M, Villabrille PI, Romanelli GP, Vazquez PG, Caceres CV (2012) Preparation, characterization and use of V_2O_5-TiO_2 mixed xerogels as catalysts for sustainable oxidation with hydrogen peroxide of 2,3,6-trimethylphenol. Appl Catal A: Gen 417-418:273–280
9. Bellardita M, García-López EI, Marcì G, Megna B, Pomilla FR, Palmisano L (2015) Photocatalytic conversion of glucose in aqueous suspensions of heteropolyacid-TiO_2 composites. RSC Adv 5:59037–59047
10. De Souza Lourenço RER, Passoni LC, Canela MC (2014) The synergistic effect of TiO_2 and $H_5PW_{10}V_2O_{40}$ in photocatalysis as a function of the irradiation source. J Mol Catal A: Chem 392:284–289
11. Fuchs VM, Soto EL, Blanco MN, Pizzio LR (2008) Direct modification with tungstophosphoric acid of mesoporous titania synthesized by urea-templated sol–gel reactions. J Colloid Interface Sci 327:403–411
12. Mercier C, Chabardes P (1994) Organometallic chemistry in industrial vitamin A and vitamin E synthesis. Pure Appl Chem 66:1509–1518
13. Gao X, An J, Gu J, Li L, Li Y (2017) A green template-assisted synthesis of hierarchical TS-1 with excellent catalytic activity and recyclability for the oxidation of 2,3,6-trimethylphenol. Micropor Mesopor Mat 239:381–389
14. Netscher T, Malaisé G, Bonrath W, Breuninger M (2007) A new route to Vitamin E key-intermediates by olefin cross-metathesis. Catal Today 121:71–75
15. Kholdeeva OA, Zalomaeva OV (2016) Recent advances in transition-metal-catalyzed selective oxidation of substituted phenols and methoxyarenes with environmentally benign oxidants. Coord Chem Rev 306:302–330
16. Packer L, WebeR SU, Rimbach G (2001) Molecular aspects of α-tocotrienol antioxidant action and cell signaling. J Nutr 131:3695–3735
17. Saux C, Pizzio LR, Pierella LB (2003) 2,3,5-Trimethylphenol oxidation over Co-based solid catalysts. Appl Catal A: Gen 452:17–23
18. Yamamura S (2003) Oxidation of phenols. Rappoport Z (ed). Willey, New York
19. Hu MSL, Yu J, Xin H, An Z, Sun W (2017) Aerobic water–based oxidation of 2,3,6-trimethylphenol to trimethyl-1,4-benzoquinone over Copper(II) Nitrate catalyst. Chem Sel 2:949–952
20. Kozhevnikov IV (1998) Catalysis by heteropoly acids and multicomponent polyoxometalates in liquid-phase reactions. Chem Rev 98:171–198
21. Evtushok VY, Suboch AN, Podyacheva OY, Stonkus OA, Zaikovskii VI, Chesalov YA, Kibis LS, Kholdeeva OA (2018) Highly efficient catalysts based on divanadium-substituted polyoxometalate and N-doped carbon nanotubes for selective oxidation of alkylphenols. ACS Catal 8:1297–1307
22. Arends IWCE, Sheldon RA (2002) Recent developments in selective catalytic epoxidations with H_2O_2. Top Catal 19:133–134
23. Koreniuk A, Maresz K, Odrozek K, Mrowiec-Białon J (2016) Titania-silica monolithic multichannel microreactors. Proof of concept and fabrication/structure/catalytic properties in the oxidation of 2,3,6-trimethylphenol. Micropor Mesopor Mat 229:98–105
24. Torbina VV, Vodyankin AA, Ivanchikov ID, Kholdeeva OA, Vodyankina OV (2015) Support pretreatment effect on the catalytic properties and reusability of silica-supported titania catalysts in 2,3,6-trimethylphenol oxidation with hydrogen peroxide. Kinet Catal 56:370–376
25. Mikushina YU, Shishmakov AB, Petrov LA (2017) Oxidation of 2,3,6-trimethylphenol to 2,3,5-trimethyl-1,4-benzoquinone over binary xerogels TiO_2-SiO_2 in the three-phase system. Russ Chem Bull 66:677–682
26. Ivanchikova ID, Maksimchuk NV, Maksimovskaya RL, Maksimov GM, Kholdeeva OA (2014) Highly selective oxidation of alkylphenols to p-benzoquinones with aqueous hydrogen peroxide catalyzed by divanadium-substituted polyoxotungstates. ACS Catal 4:2706–2713
27. Villabrille P, Romanelli G, Vázquez P, Cáceres C (2004) Vanadium-substituted Keggin heteropolycompounds as catalysts for ecofriendly liquid phase oxidation of 2,6-dimethylphenol to 2,6-dimethyl-1,4-benzoquinone. Appl Catal A: Gen 270:101–111
28. Mayani SV, Mayani VJ, Wook Kim S (2013) Synthesis of molybdovanadophosphoric acid supported hybrid materials and their heterogeneous catalytic activity. Mater Lett 111:112–115
29. Nur H, Hau NY, Misnon II, Hamdan H, Muhid MNM (2006) Hydrophobic fluorinated TiO_2–ZrO_2 as catalyst in epoxidation of 1-octene with aqueous hydrogen peroxide. Mater Lett 60:2274–2277
30. Concellón A, Vázquez P, Blanco M, Cáceres C (1998) Molybdophosphoric acid adsorption on titania from ethanol–water solutions. J Colloid Interface Sci 204:256–267
31. Khalameida SV, Sydorchuk VV, Skubiszewska-Zieba J, Leboda R, Zazhigalov VA (2014) Sol-gel synthesis and properties of compositions containing heteropoly compounds in porous silica matrix. Glass Phys Chem 40:8–16
32. Cid R, Pecchi G (1985) Potentiometric method for determining the number and relative strength of acid sites in colored catalysts. Appl Catal 14:15–21
33. Palermo V, Sathicq ÁG, Vázquez PG, Thomas HJ (2011) Doped Keggin heteropolyacids as catalysts in sulfide oxidation. Reac Kinet Mech Cat 104:181–195
34. Villabrille P, Romanelli GP, Vázquez P, Cáceres C (2008) Supported heteropolycompounds as ecofriendly catalysts for 2,6-dimethylphenol oxidation to 2,6-dimethyl-1,4-benzoquinone. Appl Catal A: Gen 334:374–380
35. Benadji S, Eloy P, Leonard A, Su B-L, Rabia C, Gaigneaux EM (2012) Characterization of $H_{3+x}PMo_{12-x}V_xO_{40}$ heteropolyacids supported on HMS mesoporous molecular sieve and their catalytic performance in propene oxidation. Micropor Mesopor Mat 154:153–163
36. Predoeva A, Damyanova S, Gaigneaux EM, Petrov L (2007) The surface and catalytic properties of titania-supported mixed PMoV

heteropoly compounds for total oxidation of chlorobenzene. Appl Catal A: Gen 319:14–24
37. Klissurski O, Hadjiivanov K, Kantcheva M, Gyurova L (1990) Study of peroxide-modified titanium dioxide (Anatase). J Chem Soc Faraday Trans 86:385–388
38. Arends IWCE, Sheldon RA (2001) Activities and stabilities of heterogeneous catalysts in selective liquid phase oxidations: recent developments. Appl Catal A: Gen 212: 175–187
39. Li K, Yang X, Guo Y, Ma F, Li H, Chen L, Guo Y (2010) Design of mesostructured $H_3PW_{12}O_{40}$–titania materials with controllable structural orderings and pore geometries and their simulated sunlight photocatalytic activity towards diethyl phthalate degradation. Appl Catal B: Environ 99:364–375